J/ψ Production and Nuclear Effects for $d+Au$ and $p+p$ Collisions at $\sqrt{s_{NN}} = 200$ GeV

S.S. Adler,[5] S. Afanasiev,[20] C. Aidala,[10] N.N. Ajitanand,[44] Y. Akiba,[21,40] A. Al-Jamel,[35] J. Alexander,[44] K. Aoki,[25] L. Aphecetche,[46] R. Armendariz,[35] S.H. Aronson,[5] R. Averbeck,[45] T.C. Awes,[36] V. Babintsev,[17] A. Baldisseri,[11] K.N. Barish,[6] P.D. Barnes,[28] B. Bassalleck,[34] S. Bathe,[6,31] S. Batsouli,[10] V. Baublis,[39] F. Bauer,[6] A. Bazilevsky,[5,41] S. Belikov,[19,17] M.T. Bjorndal,[10] J.G. Boissevain,[28] H. Borel,[11] M.L. Brooks,[28] D.S. Brown,[35] N. Bruner,[34] D. Bucher,[31] H. Buesching,[5,31] V. Bumazhnov,[17] G. Bunce,[5,41] J.M. Burward-Hoy,[28,27] S. Butsyk,[45] X. Camard,[46] P. Chand,[4] W.C. Chang,[2] S. Chernichenko,[17] C.Y. Chi,[10] J. Chiba,[21] M. Chiu,[10] I.J. Choi,[53] R.K. Choudhury,[4] T. Chujo,[5] V. Cianciolo,[36] Y. Cobigo,[11] B.A. Cole,[10] M.P. Comets,[37] P. Constantin,[19] M. Csanád,[13] T. Csörgő,[22] J.P. Cussonneau,[46] D. d'Enterria,[10] K. Das,[14] G. David,[5] F. Deák,[13] H. Delagrange,[46] A. Denisov,[17] A. Deshpande,[41] E.J. Desmond,[5] A. Devismes,[45] O. Dietzsch,[42] J.L. Drachenberg,[1] O. Drapier,[26] A. Drees,[45] A. Durum,[17] D. Dutta,[4] V. Dzhordzhadze,[47] Y.V. Efremenko,[36] H. En'yo,[40,41] B. Espagnon,[37] S. Esumi,[49] D.E. Fields,[34,41] C. Finck,[46] F. Fleuret,[26] S.L. Fokin,[24] B.D. Fox,[41] Z. Fraenkel,[52] J.E. Frantz,[10] A. Franz,[5] A.D. Frawley,[14] Y. Fukao,[25,40,41] S.-Y. Fung,[6] S. Gadrat,[29] M. Germain,[46] A. Glenn,[47] M. Gonin,[26] J. Gosset,[11] Y. Goto,[40,41] R. Granier de Cassagnac,[26] N. Grau,[19] S.V. Greene,[50] M. Grosse Perdekamp,[18,41] H.-Å. Gustafsson,[30] T. Hachiya,[16] J.S. Haggerty,[5] H. Hamagaki,[8] A.G. Hansen,[28] E.P. Hartouni,[27] M. Harvey,[5] K. Hasuko,[40] R. Hayano,[8] X. He,[15] M. Heffner,[27] T.K. Hemmick,[45] J.M. Heuser,[40] P. Hidas,[22] H. Hiejima,[18] J.C. Hill,[19] R. Hobbs,[34] W. Holzmann,[44] K. Homma,[16] B. Hong,[23] A. Hoover,[35] T. Horaguchi,[40,41,48] T. Ichihara,[40,41] V.V. Ikonnikov,[24] K. Imai,[25,40] M. Inaba,[49] M. Inuzuka,[8] D. Isenhower,[1] L. Isenhower,[1] M. Ishihara,[40] M. Issah,[44] A. Isupov,[20] B.V. Jacak,[45] J. Jia,[45] O. Jinnouchi,[40,41] B.M. Johnson,[5] S.C. Johnson,[27] K.S. Joo,[32] D. Jouan,[37] F. Kajihara,[8] S. Kametani,[8,51] N. Kamihara,[40,48] M. Kaneta,[41] J.H. Kang,[53] K. Katou,[51] T. Kawabata,[8] A.V. Kazantsev,[24] S. Kelly,[9,10] B. Khachaturov,[52] A. Khanzadeev,[39] J. Kikuchi,[51] D.J. Kim,[53] E. Kim,[43] G.-B. Kim,[26] H.J. Kim,[53] E. Kinney,[9] A. Kiss,[13] E. Kistenev,[5] A. Kiyomichi,[40] C. Klein-Boesing,[31] H. Kobayashi,[41] L. Kochenda,[39] V. Kochetkov,[17] R. Kohara,[16] B. Komkov,[39] M. Konno,[49] D. Kotchetkov,[6] A. Kozlov,[52] P.J. Kroon,[5] C.H. Kuberg,[1] G.J. Kunde,[28] K. Kurita,[40] M.J. Kweon,[23] Y. Kwon,[53] G.S. Kyle,[35] R. Lacey,[44] J.G. Lajoie,[19] Y. Le Bornec,[37] A. Lebedev,[19,24] S. Leckey,[45] D.M. Lee,[28] M.J. Leitch,[28] M.A.L. Leite,[42] X.H. Li,[6] H. Lim,[43] A. Litvinenko,[20] M.X. Liu,[28] C.F. Maguire,[50] Y.I. Makdisi,[5] A. Malakhov,[20] V.I. Manko,[24] Y. Mao,[38,40] G. Martinez,[46] H. Masui,[49] F. Matathias,[45] T. Matsumoto,[8,51] M.C. McCain,[1] P.L. McGaughey,[28] Y. Miake,[49] T.E. Miller,[50] A. Milov,[45] S. Mioduszewski,[5] G.C. Mishra,[15] J.T. Mitchell,[5] A.K. Mohanty,[4] D.P. Morrison,[5] J.M. Moss,[28] D. Mukhopadhyay,[52] M. Muniruzzaman,[6] S. Nagamiya,[21] J.L. Nagle,[9,10] T. Nakamura,[16] J. Newby,[47] A.S. Nyanin,[24] J. Nystrand,[30] E. O'Brien,[5] C.A. Ogilvie,[19] H. Ohnishi,[40] I.D. Ojha,[3,50] H. Okada,[25,40] K. Okada,[40,41] A. Oskarsson,[30] I. Otterlund,[30] K. Oyama,[8] K. Ozawa,[8] D. Pal,[52] A.P.T. Palounek,[28] V. Pantuev,[45] V. Papavassiliou,[35] J. Park,[43] W.J. Park,[23] S.F. Pate,[35] H. Pei,[19] V. Penev,[20] J.-C. Peng,[18] H. Pereira,[11] V. Peresedov,[20] A. Pierson,[34] C. Pinkenburg,[5] R.P. Pisani,[5] M.L. Purschke,[5] A.K. Purwar,[45] J.M. Qualls,[1] J. Rak,[19] I. Ravinovich,[52] K.F. Read,[36,47] M. Reuter,[45] K. Reygers,[31] V. Riabov,[39] Y. Riabov,[39] G. Roche,[29] A. Romana,[26] M. Rosati,[19] S.S.E. Rosendahl,[30] P. Rosnet,[29] V.L. Rykov,[40] S.S. Ryu,[53] N. Saito,[25,40,41] T. Sakaguchi,[8,51] S. Sakai,[49] V. Samsonov,[39] L. Sanfratello,[34] R. Santo,[31] H.D. Sato,[25,40] S. Sato,[5,49] S. Sawada,[21] Y. Schutz,[46] V. Semenov,[17] R. Seto,[6] T.K. Shea,[5] I. Shein,[17] T.-A. Shibata,[40,48] K. Shigaki,[16] M. Shimomura,[49] A. Sickles,[45] C.L. Silva,[42] D. Silvermyr,[28] K.S. Sim,[23] A. Soldatov,[17] R.A. Soltz,[27] W.E. Sondheim,[28] S.P. Sorensen,[47] I.V. Sourikova,[5] F. Staley,[11] P.W. Stankus,[36] E. Stenlund,[30] M. Stepanov,[35] A. Ster,[22] S.P. Stoll,[5] T. Sugitate,[16] J.P. Sullivan,[28] S. Takagi,[49] E.M. Takagui,[42] A. Taketani,[40,41] K.H. Tanaka,[21] Y. Tanaka,[33] K. Tanida,[40] M.J. Tannenbaum,[5] A. Taranenko,[44] P. Tarján,[12] T.L. Thomas,[34] M. Togawa,[25,40] J. Tojo,[40] H. Torii,[25,41] R.S. Towell,[1] V-N. Tram,[26] I. Tserruya,[52] Y. Tsuchimoto,[16] E. Tujuba,[26] H. Tydesjö,[30] N. Tyurin,[17] T.J. Uam,[32] J. Velkovska,[5] M. Velkovsky,[45] V. Veszprémi,[12] A.A. Vinogradov,[24] M.A. Volkov,[24] E. Vznuzdaev,[39] X.R. Wang,[15] Y. Watanabe,[40,41] S.N. White,[5] N. Willis,[37] F.K. Wohn,[19] C.L. Woody,[5] W. Xie,[6] A. Yanovich,[17] S. Yokkaichi,[40,41] G.R. Young,[36] I.E. Yushmanov,[24] W.A. Zajc,[10,*] C. Zhang,[10] S. Zhou,[7] J. Zimányi,[22] L. Zolin,[20] X. Zong,[19] and H.W. vanHecke[28]

(PHENIX Collaboration)

[1] *Abilene Christian University, Abilene, TX 79699, USA*
[2] *Institute of Physics, Academia Sinica, Taipei 11529, Taiwan*
[3] *Department of Physics, Banaras Hindu University, Varanasi 221005, India*
[4] *Bhabha Atomic Research Centre, Bombay 400 085, India*

[5]Brookhaven National Laboratory, Upton, NY 11973-5000, USA
[6]University of California - Riverside, Riverside, CA 92521, USA
[7]China Institute of Atomic Energy (CIAE), Beijing, People's Republic of China
[8]Center for Nuclear Study, Graduate School of Science, University of Tokyo, 7-3-1 Hongo, Bunkyo, Tokyo 113-0033, Japan
[9]University of Colorado, Boulder, CO 80309, USA
[10]Columbia University, New York, NY 10027 and Nevis Laboratories, Irvington, NY 10533, USA
[11]Dapnia, CEA Saclay, F-91191, Gif-sur-Yvette, France
[12]Debrecen University, H-4010 Debrecen, Egyetem tér 1, Hungary
[13]ELTE, Eötvös Loránd University, H - 1117 Budapest, Pázmány P. s. 1/A, Hungary
[14]Florida State University, Tallahassee, FL 32306, USA
[15]Georgia State University, Atlanta, GA 30303, USA
[16]Hiroshima University, Kagamiyama, Higashi-Hiroshima 739-8526, Japan
[17]IHEP Protvino, State Research Center of Russian Federation, Institute for High Energy Physics, Protvino, 142281, Russia
[18]University of Illinois at Urbana-Champaign, Urbana, IL 61801, USA
[19]Iowa State University, Ames, IA 50011, USA
[20]Joint Institute for Nuclear Research, 141980 Dubna, Moscow Region, Russia
[21]KEK, High Energy Accelerator Research Organization, Tsukuba, Ibaraki 305-0801, Japan
[22]KFKI Research Institute for Particle and Nuclear Physics of the Hungarian Academy of Sciences (MTA KFKI RMKI), H-1525 Budapest 114, POBox 49, Budapest, Hungary
[23]Korea University, Seoul, 136-701, Korea
[24]Russian Research Center "Kurchatov Institute", Moscow, Russia
[25]Kyoto University, Kyoto 606-8502, Japan
[26]Laboratoire Leprince-Ringuet, Ecole Polytechnique, CNRS-IN2P3, Route de Saclay, F-91128, Palaiseau, France
[27]Lawrence Livermore National Laboratory, Livermore, CA 94550, USA
[28]Los Alamos National Laboratory, Los Alamos, NM 87545, USA
[29]LPC, Université Blaise Pascal, CNRS-IN2P3, Clermont-Fd, 63177 Aubiere Cedex, France
[30]Department of Physics, Lund University, Box 118, SE-221 00 Lund, Sweden
[31]Institut für Kernphysik, University of Muenster, D-48149 Muenster, Germany
[32]Myongji University, Yongin, Kyonggido 449-728, Korea
[33]Nagasaki Institute of Applied Science, Nagasaki-shi, Nagasaki 851-0193, Japan
[34]University of New Mexico, Albuquerque, NM 87131, USA
[35]New Mexico State University, Las Cruces, NM 88003, USA
[36]Oak Ridge National Laboratory, Oak Ridge, TN 37831, USA
[37]IPN-Orsay, Universite Paris Sud, CNRS-IN2P3, BP1, F-91406, Orsay, France
[38]Peking University, Beijing, People's Republic of China
[39]PNPI, Petersburg Nuclear Physics Institute, Gatchina, Leningrad region, 188300, Russia
[40]RIKEN (The Institute of Physical and Chemical Research), Wako, Saitama 351-0198, JAPAN
[41]RIKEN BNL Research Center, Brookhaven National Laboratory, Upton, NY 11973-5000, USA
[42]Universidade de São Paulo, Instituto de Física, Caixa Postal 66318, São Paulo CEP05315-970, Brazil
[43]System Electronics Laboratory, Seoul National University, Seoul, South Korea
[44]Chemistry Department, Stony Brook University, Stony Brook, SUNY, NY 11794-3400, USA
[45]Department of Physics and Astronomy, Stony Brook University, SUNY, Stony Brook, NY 11794, USA
[46]SUBATECH (Ecole des Mines de Nantes, CNRS-IN2P3, Université de Nantes) BP 20722 - 44307, Nantes, France
[47]University of Tennessee, Knoxville, TN 37996, USA
[48]Department of Physics, Tokyo Institute of Technology, Oh-okayama, Meguro, Tokyo 152-8551, Japan
[49]Institute of Physics, University of Tsukuba, Tsukuba, Ibaraki 305, Japan
[50]Vanderbilt University, Nashville, TN 37235, USA
[51]Waseda University, Advanced Research Institute for Science and Engineering, 17 Kikui-cho, Shinjuku-ku, Tokyo 162-0044, Japan
[52]Weizmann Institute, Rehovot 76100, Israel
[53]Yonsei University, IPAP, Seoul 120-749, Korea

(Dated: July 28, 2005)

J/ψ production in $d+Au$ and $p+p$ collisions at $\sqrt{s_{NN}} = 200$ GeV has been measured by the PHENIX experiment at rapidities $-2.2 < y < +2.4$. The cross sections and nuclear dependence of J/ψ production versus rapidity, transverse momentum, and centrality are obtained and compared to lower energy $p+A$ results and to theoretical models. The observed nuclear dependence in $d+Au$ collisions is found to be modest, suggesting that the absorption in the final state is weak and the shadowing of the gluon distributions is small and consistent with DGLAP-based parameterizations that fit deep-inelastic scattering and Drell-Yan data at lower energies.

PACS numbers: 25.75.Dw

J/ψ production in hadron collisions, since it proceeds predominantly through diagrams involving gluons (e.g.

gluon fusion) [1], is a sensitive probe of the gluon structure function in the nucleon and its modification in nuclei. It is also a leading signal for the creation of hot-dense matter in heavy-ion collisions [2]. Shadowing of partons (quarks or gluons) in nuclei is a depletion of their population at small momentum fraction compared to that of a free nucleon. In $\sqrt{s_{NN}} = 200$ GeV deuteron-gold ($d+Au$) collisions at the Relativistic Heavy Ion Collider (RHIC), for forward (deuteron direction) rapidities, gluons in Au are probed that lie well into the shadowing region with momentum fractions, $x_{Au} \sim 3 \times 10^{-3}$. Leading models of gluon shadowing predict suppressions of J/ψ production in nuclei that differ by as much as a factor of three [3–5]. Recent theoretical developments, e.g. as in the Color Glass Condensate model [6], suggest that at very low fractional momenta non-linear gluon saturation effects become important and cause substantial modifications of the gluon densities.

Other expected nuclear effects on J/ψ production include energy loss and multiple scattering of the initial gluons and absorption of the $c\bar{c}$ in the final state [7]. However, this energy loss is expected to be small at RHIC energies [5]. Theoretical analysis of these effects is challenging given the poorly known production mechanism and configuration of the final-state $c\bar{c}$ [1]; and that approximately a third of the J/ψ 's come from decays of higher-mass resonances [8].

Here we present measurements made by the PHENIX experiment at RHIC for the production of J/ψ 's in $\sqrt{s_{NN}} = 200$ GeV $d+Au$ and proton-proton ($p+p$) collisions. These data provide the first nuclear dependence measurements at this energy, a much higher energy than previous measurements from fixed-target experiments at $\sqrt{s_{NN}} \lesssim 40$ GeV [9–13]. Besides the shadowing region at small x these data also probe large gluon momentum fractions (at negative rapidity) nearer the rest frame of the residual nucleus. Finally, these measurements also serve as a baseline for the upcoming results from the high-luminosity $Au+Au$ and $Cu+Cu$ runs and must be understood in order to look for effects beyond what is expected from cold nuclear matter, such as the creation of a Quark Gluon Plasma [2].

The measurements described here are similar to earlier ones with PHENIX for $p+p$ [14] and $Au+Au$ [15] collisions, but with a second muon spectrometer added and higher luminosity. The two muon spectrometers are especially valuable for asymmetric collisions such as $d+Au$ where simultaneous measurements at forward ($1.2 < y < 2.4$) and backward ($-2.2 < y < -1.2$) rapidities, along with central ($|y| \leq 0.35$) rapidity from e^+e^-, are then available. Electrons in the central arms are identified by matching charged particle tracks to clusters in an electromagnetic calorimeter (EMC) and to rings in a ring imaging Čerenkov (RICH) detector. Muons are identified by their detection in Iarocci tubes after their penetration through 6.5 to 8.5 interaction lengths of copper and steel absorber.

The data used in this analysis were recorded in 2003 using a trigger that required hits in each of the two beam-beam counters located at negative and positive rapidity ($3 < |\eta| < 3.9$). In addition, for the di-muons at least two tracks in the muon identifier of appropriate absorber depth were required, while for the di-electrons a one-track trigger with a signal above threshold in the EMC with a matching hit in the RICH was required. After quality and vertex cuts, the samples for the three arms correspond to integrated luminosities from 180 to 250 nb^{-1} ($p+p$) and 1.4 to 1.7 nb^{-1} ($d+Au$).

For the di-muons the J/ψ yield is obtained after subtraction of the combinatoric background using like-sign muon pairs ($2\sqrt{N_{++} * N_{--}}$) and by fitting the resulting mass peak with a Gaussian plus an exponential to represent the small remaining continuum background underneath the peak. A variety of continuum shapes were checked for each fit in order to establish the uncertainty due to the low-statistics background. For the di-electrons the combinatoric background was subtracted using the sum of like-sign pairs and the J/ψ yield was taken as all remaining events in the mass range 2.6 to 3.6 GeV/c^2. Approximately 2100 and 500 J/ψ's were obtained in the $\mu\mu$ and ee channels, respectively.

The differential cross sections are calculated as,

$$B_{ll}\frac{d\sigma_{J/\psi}}{dy} = \frac{N_{J/\psi}}{A\,\epsilon_{rec}\,\epsilon_{trig}\,\epsilon^{BBC}_{J/\psi}\,(N_{evt}/(\sigma^{tot}_{MB}\cdot\epsilon^{BBC}_{MB}))}\,\frac{1}{\Delta y} \quad (1)$$

and the nuclear modification factor, R_{dA}, is

$$R_{dA} = \frac{d\sigma^{dAu}_{J/\psi}/dy}{(2\times 197)\times d\sigma^{pp}_{J/\psi}/dy} \quad (2)$$

In the above expressions B_{ll} is the J/ψ branching ratio to di-leptons, $N_{J/\psi}$ is the measured J/ψ yield, A is the geometrical acceptance, ϵ_{rec} is the di-lepton reconstruction efficiency, ϵ_{trig} is the trigger efficiency, N_{evt} the number of min-bias triggers sampled, σ^{tot}_{MB} the total minimum-bias (MB) cross section, Δy is the rapidity bin width, and ϵ^{BBC}_{MB} and ϵ^{BBC}_{MB} are the beam-beam trigger efficiencies for min-bias and J/ψ events respectively. The factor of 2×197 causes R_{dA} to be one if the $d+A$ cross section is just additive from $p+p$, i.e. if there are no nuclear modifications.

For $d+Au$ collisions, the centrality of the collision can be characterized by measuring the charge deposited in the beam-beam counter in the Au beam direction [16]. An approximate number of nucleon+nucleon collisions $\langle N_{coll}\rangle$ can be obtained through a Glauber calculation that relates this $\langle N_{coll}\rangle$ to the observed charge. In this case $R_{dA}(N_{coll})$ is calculated as,

$$R_{dA}(\langle N_{coll}\rangle) = \frac{N^{dAu}_{inv}(\langle N_{coll}\rangle)}{\langle N_{coll}\rangle\times N^{pp}_{inv}} \quad (3)$$

where the invariant yield N_{inv} is,

$$N_{inv}(\langle N_{coll}\rangle) = \frac{N_{J/\psi} \cdot C_{bias}(\langle N_{coll}\rangle)}{A\,\epsilon_{rec}\,\epsilon_{trig}[N_{evt} \cdot (\Delta w/w)]} \quad (4)$$

with $\langle N_{coll}\rangle$ being the average number of binary collisions for a particular $d+Au$ centrality bin and $N_{evt} \cdot (\Delta w/w)$ the number of $d+Au$ min-bias triggers sampled that lie in this fraction, Δw, of the total minimum-bias centrality range, w. For $p+p$ collisions $\Delta w/w$ is one. $C_{bias} = \epsilon^{BBC}_{MB}/\epsilon^{BBC}_{J/\psi}$ is a correction for the smaller trigger efficiency in minimum-bias events compared to those with a J/ψ. For $d+Au$, C_{bias} depends on $\langle N_{coll}\rangle$ and takes into account the effect of the underlying event multiplicity on both the trigger efficiency and the centrality measurement [16]. Its variation with centrality is up to 7% from unity.

To complete the calculation of the $p+p$ absolute cross sections we use the cross section for our beam-beam trigger, $\sigma^{tot}_{MB}(pp) \cdot \epsilon^{BBC}_{MB}(pp) = 23.0 \pm 2.2$ mb; and the efficiency for events with a J/ψ, $\epsilon^{BBC}_{J/\psi}(pp) = 0.79 \pm 0.02$ [14]. For $d+Au$ collisions we use a beam-beam trigger cross section of $\sigma^{tot}_{MB}(dAu) \cdot \epsilon^{BBC}_{MB}(dAu) = 1.99 \pm 0.1\ b$ from our measurement [17] using photo-dissociation of the deuteron as a reference [18], which is consistent with our calculated Glauber result of $1.92 \pm 0.18\ b$. For the J/ψ we use $\epsilon^{BBC}_{J/\psi}(dAu) = 0.94 \pm 0.02$ [16].

For the electron analysis, $A\,\epsilon_{rec}$ and ϵ_{trig} were determined using a GEANT [19] simulation of the central arms and a trigger response software emulation [14]. ϵ_{rec} was confirmed by studying pairs identified as photon conversions in the data. The systematic uncertainty of 10.4% is dominated by run-to-run efficiencies (5%), yield extraction (5%), and the occupancy dependence of the efficiency (4.4%).

For the muon arms, $A\,\epsilon_{rec}\,\epsilon_{trig}$ was determined within each rapidity and p_T bin, using a GEANT simulation with J/ψ events generated by PYTHIA [20] using GRV98LO parton distribution functions. The systematic error includes discrepancies between Monte Carlo and real detector response, run-to-run variations in the detector state, and uncertainties in the PYTHIA distributions. The dominant systematic uncertainties in our result are +6/-9% from the muon identifier efficiency and up to 10% (for the most central negative rapidity $d+Au$ data) from the combinatoric background.

In Fig. 1a, we show the measured $p+p$ differential cross section times branching ratio versus rapidity with a di-electron point at mid-rapidity and two di-muon points at negative and positive rapidities. A fit to a shape generated with PYTHIA is performed and, using a di-lepton branching ratio of 5.9% [21], gives a total cross section $\sigma^{J/\psi}_{pp} = 2.61 \pm 0.20(\text{fit}) \pm 0.26(\text{abs})\ \mu$b. Variations in the parton distribution functions and models used to determine the shape are negligible compared to the fit errors. This result is smaller by about two sigma than our previous lower statistics result [14].

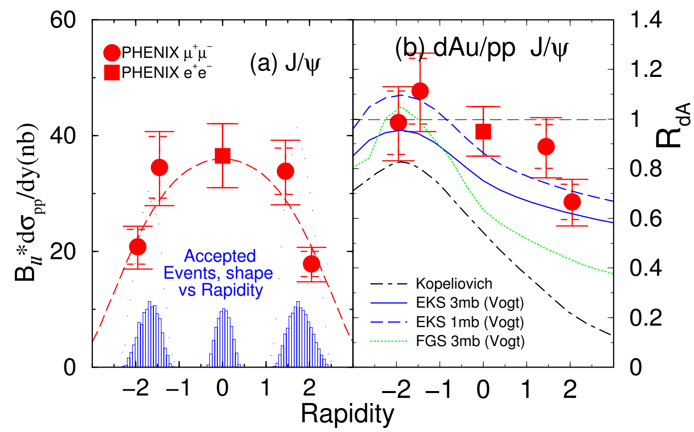

FIG. 1: (color online) (a) The 200 GeV J/ψ $p+p$ differential cross section times di-lepton branching ratio versus rapidity (10% overall normalization uncertainty is not included). (b) The minimum bias R_{dA} versus rapidity (12% overall normalization uncertainty not included). For both panels the dashed error bars represent systematic uncertainties relevant for comparing the two rapidity bins in each muon arm, while the solid error bars represent the overall uncertainties relevant for comparing points at negative, central, or positive rapidity. The curve in (a) represents a fit as described in the text while the curves in (b) are theoretical calculations [5, 22, 23] as described in the text.

The nuclear modification factor R_{dA} (Eq. 2) is shown versus rapidity in Fig. 1b, where a value of one would correspond to no nuclear modification. While this ratio is consistent with unity at backward rapidity, it is significantly lower at the most forward rapidity where gluons are expected to be shadowed in a heavy nucleus. Theoretical predictions [5, 22, 23] that include the effects of absorption and shadowing are shown for comparison in Fig. 1. The data favor a relatively modest shadowing in agreement with the parametrization of EKS98 [3] based on a leading-twist DGLAP-evolved parametrization of nuclear deep inelastic scattering and Drell-Yan data at lower energies, rather than the stronger gluon shadowing of Kopeliovich [5] or FGS [4] based on models involving coherence for a $q\bar{q}$ dipole in the nucleus. Sensitivity to the $c\bar{c}$ absorption cross section (3 or 1 mb), with the present statistical errors, is marginal.

On the other hand, if one compares to results from lower energy measurements, as shown in Fig. 2a, the suppression does not scale with the momentum fraction in the nucleus ($x_A = 0.5(-x_F + \sqrt{x_F^2 + 4M^2/s})$), as one would expect if shadowing was dominant at all energies. Here we use α, defined as $\sigma_{dA} = \sigma_{pp} \times (2A)^{\alpha}$, an often used parameter that allows for comparison of measurements made with different nuclear targets. In Fig. 2b, as was observed previously [10], the lower energy mea-

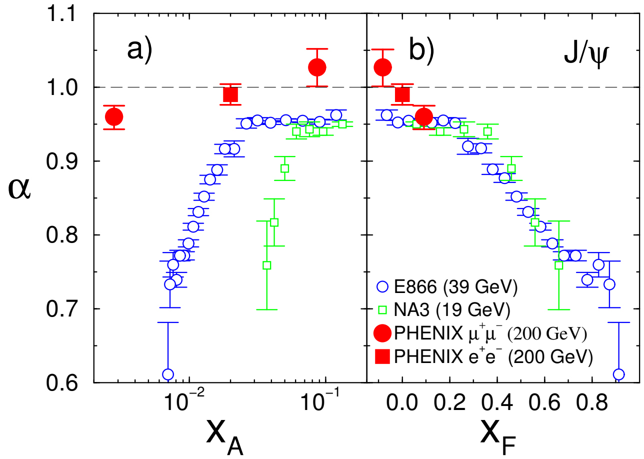

FIG. 2: (color online) α versus (a) x_A and (b) x_F with present 200 GeV J/ψ results compared to lower energy results [10, 13]. An additional overall uncertainty of 0.02 in our α values is not shown.

surements with broad x_F coverage appear to scale with $x_F = x_p - x_A$. However our results, with their limited x_F range, do not allow verification of this scaling at large x_F and have a steep rise in the low x_F region where the lower energy measurements are flat. Note that our weaker overall suppression near $x_F \sim 0$ could be due to a weaker absorption compared to that at lower energies.

It is also of interest that our nuclear dependence ratios are similar to those that were observed for charged hadrons [16, 24] in $d + Au$ collisions, where a ratio near one was seen at negative and mid-rapidity, while a value of about 0.75 was seen at forward rapidity.

Our invariant cross sections versus transverse momentum, $(d^2\sigma/dydp_T)/(2\pi p_T)$, have been fit to the form $A \times (1 + (p_T/B)^2)^{-6}$ [25]. Average p_T^2 values resulting from these fits are 4.28 ± 0.31, 3.17 ± 0.33 and 3.63 ± 0.25 (GeV/c)^2 for $d + Au$ collisions at backward, mid, and forward rapidity, respectively; compared with 2.51 ± 0.21 and 4.20 ± 0.76 (GeV/c)^2 for forward/backward and mid rapidity $p + p$ collisions, respectively. Our observed p_T broadening is shown in Fig. 3. For negative x_F it is consistent with that of the lower energy ($\sqrt{s_{NN}} = 39$ GeV) measurements from E866/NuSea [10], but may be flatter at positive rapidity. At central rapidity no p_T broadening is seen within errors.

The centrality dependence of the nuclear modification factor R_{dA} (Eq. 3) is shown on Fig. 4 for four centrality classes and for minimum bias collisions. This classification into centrality bins for these results can only be approximate, as indicated by the overlapping histograms of N_{coll}. At forward rapidity (small x_{Au}, or the shadowing region), a weak drop for more central collisions is observed, while no significant centrality dependence is seen for backward rapidity or for central rapidity. The theoretical curves on Fig. 4 correspond to different amounts of

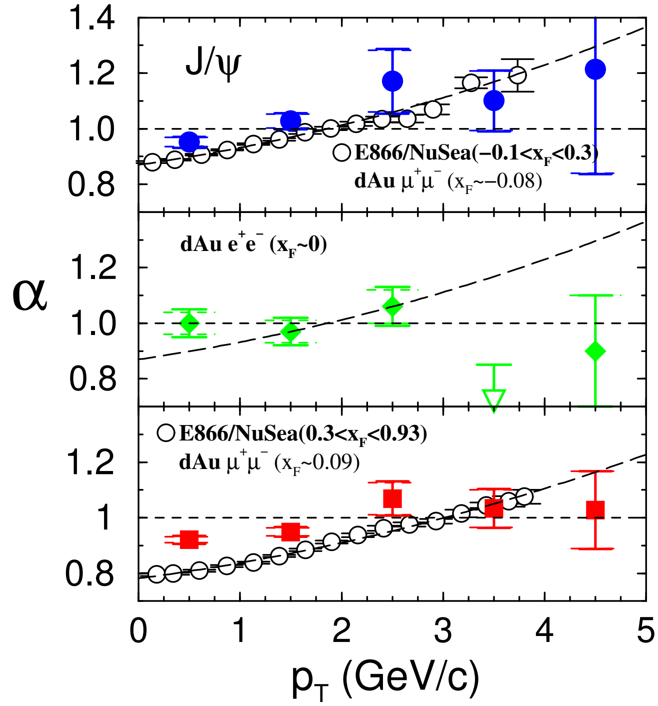

FIG. 3: (color online) α versus p_T compared to lower energy measurements, shown for three different rapidity ranges. The error bars have the same meaning as in Fig. 1. An additional 0.02 overall uncertainty is not shown. The dashed curves are simple fits [10] to the lower energy results.

density dependent shadowing and anti-shadowing [22, 23] and also include absorption. They are consistent with our data except at positive rapidity where the EKS shadowing curve is closest to our results, although slightly lower perhaps due to the amount of absorption that is included.

In summary, during the RHIC 2003 run, the PHENIX experiment measured nuclear effects on J/ψ production for $d+Au$ collisions at $\sqrt{s_{NN}} = 200$ GeV. Increasing suppression for larger rapidity (smaller x_{Au}) and for more central collisions (higher nuclear densities sampled) both are consistent with models containing a small amount of impact-parameter dependent shadowing and with weak absorption. Theoretical calculations which include EKS shadowing seem most consistent with the data. However comparisons with other measurements at lower energies show that shadowing cannot be the dominant effect, at least not for the lower energy measurements. We also see some transverse momentum broadening which is consistent with that seen at lower energy. Higher luminosity $d + Au$ running in the future yielding higher numbers of J/ψ 's will be necessary to quantify these nuclear effects and to more clearly distinguish between various theoretical models of shadowing.

We thank the staff of the Collider-Accelerator and Physics Departments at BNL for their vital contributions. We acknowledge support from the Depart-

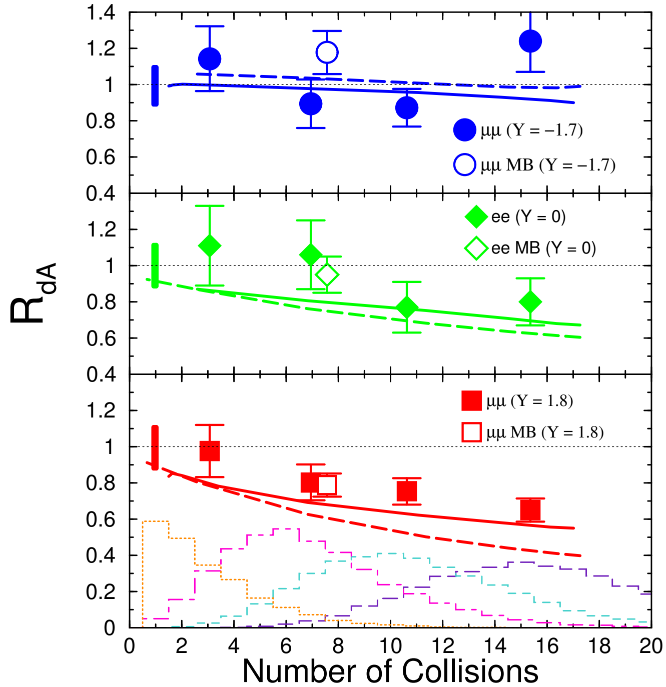

FIG. 4: (color online) Nuclear modification factor versus centrality as given by the number of nucleon-nucleon collisions shown for three different rapidity ranges, compared to theoretical calculations[22, 23] including final-state absorption and EKS (solid) or FGS (dashed) shadowing. The bars at the low end of each plot represent the systematic errors between different rapidity ranges. An additional 12% global error bar is not shown. The histograms at the bottom of the lower panel indicate the distribution of the number of collisions for each of the four centrality bins.

ment of Energy and NSF (U.S.A.), MEXT and JSPS (Japan), CNPq and FAPESP (Brazil), NSFC (China), IN2P3/CNRS, CEA, and ARMINES (France), BMBF, DAAD, and AvH (Germany), OTKA (Hungary), DAE and DST (India), ISF (Israel), KRF and CHEP (Korea), RMIST, RAS, and RMAE (Russia), VR and KAW (Sweden), U.S. CRDF for the FSU, US-Hungarian NSF-OTKA-MTA, and US-Israel BSF.

* PHENIX Spokesperson:`zajc@nevis.columbia.edu`

[1] M. Bedjidian et al. (2003).
[2] T. Matsui and H. Satz, Phys. Lett. **B178**, 416 (1986).
[3] K. J. Eskola, V. J. Kolhinen, and R. Vogt, Nucl. Phys. **A696**, 729 (2001).
[4] L. Frankfurt and M. Strikman, Eur. Phys. J. **A5**, 293 (1999).
[5] B. Kopeliovich, A. Tarasov, and J. Hüfner, Nucl. Phys. **A696**, 669 (2001).
[6] L. D. McLerran and R. Venugopalan, Phys. Rev. D **49**, 2233 (1994).
[7] R. Vogt, Phys. Rev. C **61**, 035203 (2000).
[8] L. Antoniazzi et al. Phys. Rev. Lett. **70**, 383 (1993).
[9] D. M. Alde et al., Phys. Rev. Lett. **66**, 133 (1991).
[10] M. J. Leitch et al., Phys. Rev. Lett. **84**, 3256 (2000).
[11] B. Alessandro et al., Phys. Lett. **B553**, 167 (2003).
[12] J. Spengler J. Phys. **G30**, S871 (2004).
[13] J. Badier et al., Z. Phys. **C20**, 101 (1983).
[14] S. S. Adler et al., Phys. Rev. Lett. **92**, 051802 (2004).
[15] S. S. Adler et al., Phys. Rev. C **69**, 014901 (2004).
[16] S. S. Adler et al., Phys. Rev. Lett. **94**, 082302 (2005).
[17] S. N. White, Proceedings of XIIIth International Workshop on Deep Inelastic Scattering, Madison, WI, W.H. Smith, ed. (2005), nucl-ex/0507023.
[18] S. R. Klein and R. Vogt, Phys. Rev. C **67**, 047901 (2003).
[19] *Geant 3.2.1, CERN program library* (1993).
[20] T. Sjostrand et al., Comput. Phys. Commun. **135**, 238 (2001).
[21] S. Eidelman et al., Phys. Lett. **B592**, 1 (2004).
[22] S. R. Klein and R. Vogt, Phys. Rev. Lett. **91**, 142301 (2003).
[23] R. Vogt, Phys. Rev. C **71**, 054902 (2005).
[24] B. B. Back et al., Phys. Rev. Lett. **93**, 082301 (2004).
[25] J. K. Yoh et al., Phys. Rev. Lett. **41**, 684 (1978).